J|A|C|S ARTICLES

Published on Web 05/11/2010

Using Intramolecular Energy Transfer to Transform non-Photoactive, Visible-Light-Absorbing Chromophores into Sensitizers for Photoredox Reactions

Jing Gu, Jin Chen, and Russell H. Schmehl*

Department of Chemistry, Tulane University, New Orleans, Louisiana 70118

Received November 18, 2009; E-mail: russ@tulane.edu

Abstract: This work discusses the synthesis, photophysical behavior, and photoinduced electron-transfer reactivity of multichromophoric molecules having a visible-light-absorbing MLCT component coupled to a ligand with a localized excited state of the same spin multiplicity that serves to lengthen the excited-state lifetime of the complex significantly. The appropriate ligands were prepared by Wittig coupling of a bipyridine derivative with pyrenecarboxaldehyde. The modified ligand, a pyrene-vinyl-bipyridyl ensemble (pyrv-bpy), was then reacted with $RuCl_3$ to yield $[(pyrv\text{-}bpy)_2RuCl_2]$. The complex has MLCT absorption out to 800 nm, and excitation results in the formation of a ligand-localized excited state with a lifetime long enough to undergo bimolecular electron-transfer reactions. The pyrenylvinyl "localized" excited state of the complex reacts via photoinduced electron transfer with a variety of viologen and diquat electron acceptors. The remarkable aspect of the electron-transfer process is that whereas the excited state can be considered to be ligand-localized the photoredox reaction almost certainly involves the direct formation of the one-electron-oxidized metal center.

Introduction

Transition-metal complex chromophores have been widely used as sensitizers for photoredox reactions and have become significant as sensitizers for charge injection into semiconductors in dye-sensitized solar cells.[1−6] A desired characteristic for chromophores employed in solar energy conversion schemes is that they absorb light throughout the entire visible spectrum and have excited-state energies high enough for useful light-induced redox chemistry.[7−10] Unfortunately, many complexes that absorb well in the red via metal-to-ligand charge-transfer transitions (MLCT) also have very short excited-state lifetimes that serve to diminish their utility as sensitizers for light-induced electron-transfer reactions. Reasons for the rapid nonradiative relaxation in transition-metal complex chromophores are well established and involve either relaxation through a manifold of ligand-field (LF or MC) excited states or enhanced coupling of excited-state and ground-state potential surfaces with decreasing energy gaps (energy gap law limitations).[11−14] Although there are numerous purely organic chromophores with relatively low energy triplet excited states (in the red or near-infrared) with lifetimes of microseconds or longer in solution, transition-metal complex chromophores generally have much shorter excited-state lifetimes regardless of the differences in spin between the ground and excited states because of much higher spin−orbit coupling interactions and also because of the coupling of charge transfer and ligand-field or metal-centered (LF or MC) excited states (i.e., very high density of states).[11−16] Nonetheless, the development of transition-metal complex chromophores is attractive because many complexes have fully reversible one-electron oxidation and reduction potentials, making them very useful as photoredox sensitizers, and many complexes exhibit visible absorption that can be tuned by systematic ligand variation.[3,7,9,12,15]

One approach to extending the excited-state lifetime of metal complex chromophores is to couple excited states localized on the metal complex with states of triplet spin multiplicity on a covalently linked organic (often aromatic hydrocarbon) component. The approach was demonstrated in the 1970s by Wrighton[17−20] and has been exploited in a variety of ways since

(1) Williams, J. A. G. *Top. Curr. Chem.* **2007**, *281*, 205–268.
(2) Kumaresan, D.; Shankar, K.; Vaidya, S.; Schmehl, R. H. *Top. Curr. Chem.* **2007**, *281*, 101–142.
(3) Alstrum-Acevedo, J. H.; Brennaman, M. K.; Meyer, T. J. *Inorg. Chem.* **2005**, *44*, 6802–6827.
(4) Nazeeruddin, M. K.; Gratzel, M. *Struct. Bonding (Berlin)* **2006**, *123*, 113–175.
(5) Li, B.; Wang, L.; Kang, B.; Wang, P.; Qiu, Y. *Sol. Energy Mater. Sol. Cells* **2006**, *90*, 549–573.
(6) Gust, D.; Moore, T. A.; Moore, A. L. *Acc. Chem. Res.* **2001**, *34*, 40–48.
(7) Kudo, A.; Miseki, Y. *Chem. Soc. Rev.* **2009**, *38*, 253–278.
(8) Barber, J. *Chem. Soc. Rev.* **2009**, *38*, 185–196.
(9) Ardo, S.; Meyer, G. J. *Chem. Soc. Rev.* **2009**, *38*, 115–164.
(10) Hofmeier, H.; Schubert, U. S. *Chem. Soc. Rev.* **2004**, *33*, 373–399.
(11) Meyer, T. J. *Pure Appl. Chem.* **1986**, *58*, 1193–206.
(12) Juris, A.; Balzani, V.; Barigelletti, F.; Campagna, S.; Belser, P.; Von Zelewsky, A. *Coord. Chem. Rev.* **1988**, *84*, 85–277.
(13) Chen, Y. J.; Xie, P.; Heeg, M. J.; Endicott, J. F. *Inorg. Chem.* **2006**, *45*, 6282–6297.
(14) Chen, P.; Meyer, T. J. *Chem. Rev.* **1998**, *98*, 1439–1477.
(15) Vlcek, A. *Coord. Chem. Rev.* **2000**, *200−202*, 933–978.
(16) Caspar, J. V.; Meyer, T. J. *Inorg. Chem.* **1983**, *22*, 2444–2453.
(17) Wrighton, M. S.; Morse, D. L.; Pdungsap, L. *J. Am. Chem. Soc.* **1975**, *97*, 2073–2079.
(18) Pdungsap, L.; Wrighton, M. S. *J. Organomet. Chem.* **1977**, *127*, 337–347.
(19) Giordano, P. J.; Fredericks, S. M.; Wrighton, M. S.; Morse, D. L. *J. Am. Chem. Soc.* **1978**, *100*, 2257–2259.
(20) Fredericks, S. M.; Luong, J. C.; Wrighton, M. S. *J. Am. Chem. Soc.* **1979**, *101*, 7415–7417.

10.1021/ja909785b

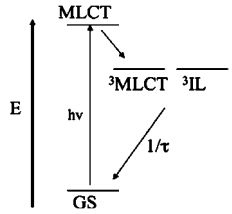

Figure 1. Energy-level diagram for complexes having nearly isoenergetic MLCT and IL triplet states.

then to yield complexes of Ru(II),[21−28] Os(II),[29,30] and Pt(II)[31,32] with very long excited-state lifetimes. Depending on the energy gap between the states involved, the system either can be in equilibrium or can be effectively localized on the pendant ligand triplet (Figure 1).[33,34] In this article, we report the exploitation of intramolecular energy transfer from MLCT excited states to the ligand-localized triplet state to achieve long-wavelength visible-light-absorbing chromophores with significant excited-state lifetime enhancements relative to that of the complex having only the MLCT state. In addition, the work illustrates that the complexes are active sensitizers for light-induced electron-transfer reactions.

The chromophores are derivatives of Ru(II) bipyridine complexes in which the bipyridine ligand has been substituted with a vinyl pyrenyl moiety (pyrv-bpy, Figure 2, Scheme 1) that provides a low-energy triplet excited state to serve as an excitation energy reservoir in the complexes. The chromophores reported here are $[(bpy)_2RuCl_2]$ and $[(bpy)_2Ru(en)](PF_6)_2$ (en = ethylenediamine) and the corresponding pyrv-bpy complexes.

Results and Discussion

Ligand and Complex Syntheses. The ligand pyrv-bpy was prepared from 4,4′-dimethyl-2,2′-bipyridine by NBS bromonation of the methyl, the formation of diethyl phosphonate from bromide, and the reaction of phosphonate with pyrene-1-carboxaldehyde under Knovenagle conditions as shown in Scheme 1. The Ru(II) cis-chloro complexes were prepared using a variation of literature methods.[35] $RuCl_3 \cdot nH_2O$ was refluxed in 2-methoxyethanol with 2 equiv of bipyridine under an Ar atmosphere for 8 h. The complex was purified by reprecipitation and characterized by UV−vis, cyclic voltammetry, and ESI mass spectrometry (HRMS). The ethylenediamine complexes were prepared from the cis-chloro derivative via reaction with excess ethylene diamine (en) in refluxing ethanol, also under Ar. The complexes were purified by reprecipitation and characterized by the above techniques.

Spectrophotometry and Electrochemistry. Absorption spectra of the cis-chloro and en complexes in acetonitrile are shown in Figures 3 and 4, along with the spectrum of $[(pyrv\text{-}bpy)_3Zn]^{2+}$. The Zn complex is included because it illustrates the absorption of the pyrv-bpy ligand when coordinated to a metal lacking MLCT or ligand-field transitions. Absorption maxima and absorbtivities are given in Table 1. Ligand pyr-bpy and complex $[(pyr\text{-}bpy)_2RuCl_2]$ are also included to illustrate the importance of the ethylene substituent in the molecule.

The transition observed near 300 nm for both ligands and all of the complexes can be readily assigned as a bipyridine-localized $\pi-\pi^*$ transition, analogous to similar transitions observed for nearly all bipyridine-containing M(II) complexes.[12] For ligand pyr-bpy, the absorption spectrum includes a pyrene-localized $\pi-\pi^*$ transition with a maximum at 342 nm, and the pyrv-bpy ligand has a maximum much farther to the red, at 390 nm, reflecting electronic interaction between pyrene and bipyridine. The long-wavelength maximum of the Zn complex at 424 nm is also a ligand-localized $\pi-\pi^*$ transition; the lower energy of the transition relative to pyrv-bpy may be related to some degree of charge-transfer character between the pyrene and the coordinated bipyridine, similar to that clearly observed and characterized in terpyridyl phenylene vinylene complexes of Zn(II).[36]

The spectra of the Ru(II) complexes have two visible absorption maxima; the longest-wavelength absorption maxi-

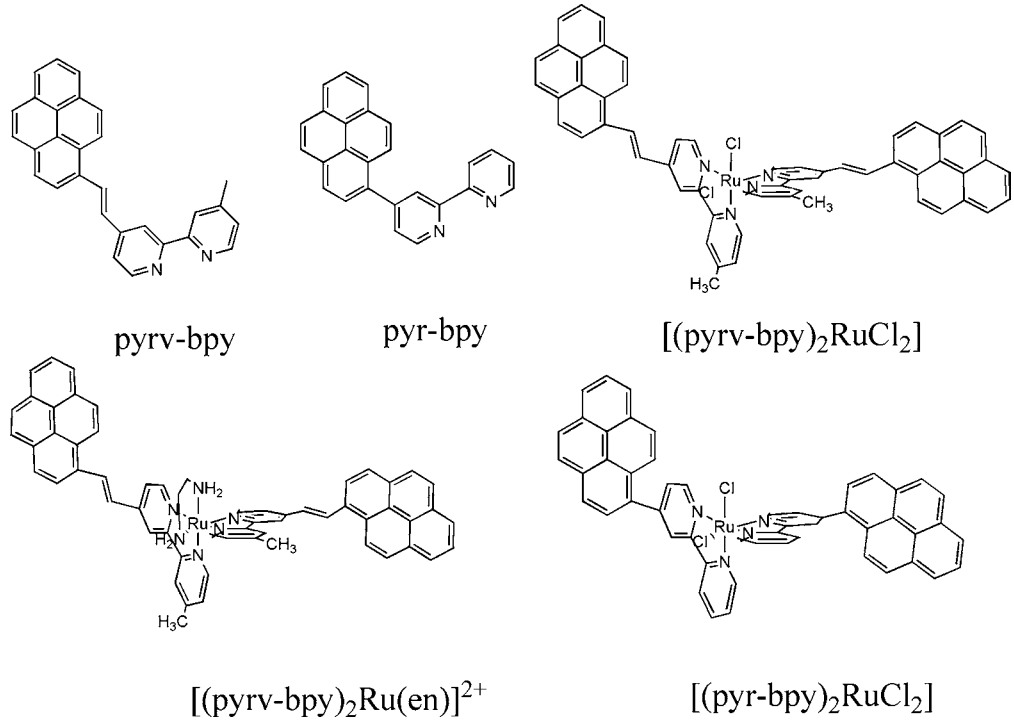

Figure 2. Representation of one stereoisomer of the pyrv-bpy and pyr-bpy ligands and the complexes.

Scheme 1. Ligand Synthesis

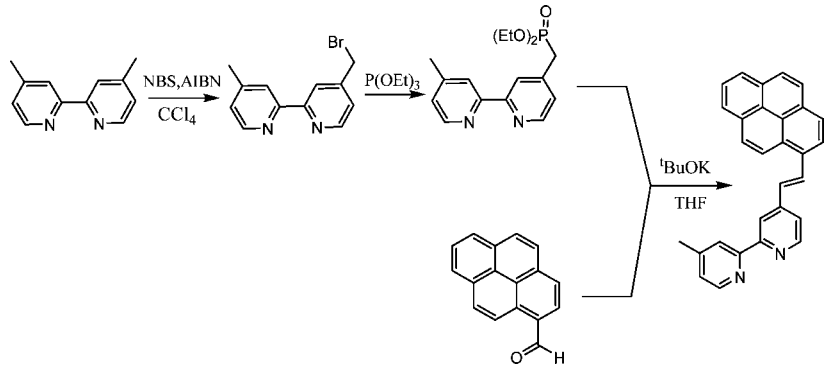

mum ($\lambda > 500$ nm) can be assigned as an MLCT transition on the basis of a literature precedent[37] and computational analysis (density functional calculations section). The absorption between 350 and 450 nm is very likely of MLCT origin for [$(bpy)_2RuCl_2$][38] but represents the overlap of the localized pyrv-bpy ligand and MLCT transitions for the pyrv-bpy complex. The absorptivity of both visible transitions is $>10^4$ $M^{-1}cm^{-1}$ for the pyrv-bpy complexes at their maxima, indicating that the transitions are strongly allowed.

The cis-chloro complexes exhibit slight solvatochromism associated with the long-wavelength MLCT absorption transition; Table 3 presents the absorption maxima for both visible transitions in a variety of solvents. The magnitude of the solvatochromism is not large, ranging from 580 nm in acetonitrile to 606 nm in benzonitrile, and the observed spectral behavior does not seem to correlate with any measure of solvent polarity such as Gutmann solvent donor or acceptor numbers or the ET(30) scale.[39]

The redox behavior of the ligands and complexes was examined in DMF solution by a combination of cyclic voltammetry and differential pulse voltammetry; potentials are included in Table 1. Ligands pyr-bpy and pyrv-bpy both exhibit irreversible oxidation (as does pyrene); the oxidation is pyrene-localized because the parent ligand, 2,2′-bipyridine (bpy), and a model for pyrv-bpy, 4-(styryl)-2,2′-bipyridine, have no oxidative waves at potentials less than +1.8 V versus SCE.[12]

The [$(bpy)_2RuCl_2$], [$(pyr\text{-}bpy)_2RuCl_2$], and [$(pyrv\text{-}bpy)_2RuCl_2$] cis-chloro complexes all exhibit reversible one-electron oxidation at <0.4 V versus SCE in acetonitrile (Table 1). On the basis of earlier work by others, the oxidation is assigned to the oxidation of Ru(II) to Ru(III).[16] The pyrene-containing complexes also have an irreversible oxidation wave in cyclic voltammograms at potentials corresponding to pyrene oxidation (1.4 to 1.6 V vs SCE).[24] All of the complexes had several overlapping quasi-reversible reductive waves between −1.4 and −2.0 V. By analogy to complexes reported in the literature, the waves correspond to the reduction of the bipyridine ligands. Complex [$(pyrv\text{-}bpy)_2RuCl_2$] was examined by spectroelectrochemistry in order to determine the spectrum of and evaluate the stability of the Ru(III) form of the complex. Figure 5 shows visible absorption spectra obtained before and after oxidation at +0.5 V (SCE). The two charge-transfer bands of the Ru(II) complex disappear, and a new transition is observed with a maximum of 435 nm. A precipitate formed during the oxidation

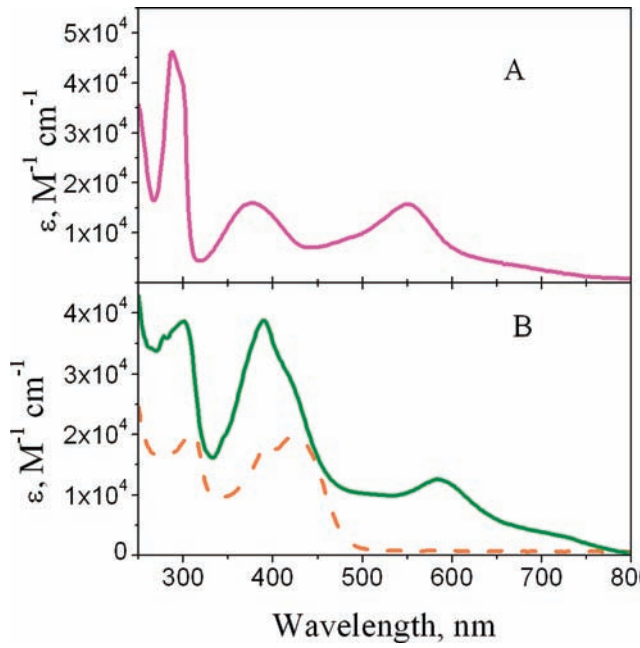

Figure 3. UV−vis absorption spectra in CH_3CN of (A) [$Ru(bpy)_2Cl_2$] and (B) $[Zn(pyrv\text{-}bpy)_3]^{2+}$ (yellow ---, $\varepsilon/5$) and [$Ru(pyrv\text{-}bpy)_2Cl_2$] (green −).

(21) Ford, W. E.; Rodgers, M. A. J. *J. Phys. Chem.* **1992**, *96*, 2917–2920.
(22) Tyson, D. S.; Castellano, F. N. *J. Phys. Chem. A* **1999**, *103*, 10955–10960.
(23) Tyson, D. S.; Castellano, F. N. Abstracts of Papers, 220th ACS National Meeting, Washington, DC, Aug 20−24, 2000.
(24) Simon, J. A.; Curry, S. L.; Schmehl, R. H.; Schatz, T. R.; Piotrowiak, P.; Jin, X.; Thummel, R. P. *J. Am. Chem. Soc.* **1997**, *119*, 11012–11022.
(25) Harriman, A.; Hissler, M.; Khatyr, A.; Ziessel, R. *Chem. Commun.* **1999**, 735–736.
(26) Hissler, M.; Harriman, A.; Khatyr, A.; Ziessel, R. *Chem.—Eur. J.* **1999**, *5*, 3366–3381.
(27) Morales, A. F.; Accorsi, G.; Armaroli, N.; Barigelletti, F.; Pope, S. J. A.; Ward, M. D. *Inorg. Chem.* **2002**, *41*, 6711–6719.
(28) Benniston, A. C.; Harriman, A.; Lawrie, D. J.; Mayeux, A. *Phys. Chem. Chem. Phys.* **2004**, *6*, 51–57.
(29) Maubert, B.; McClenaghan, N. D.; Indelli, M. T.; Campagna, S. *J. Phys. Chem. A* **2003**, *107*, 447–455.
(30) Balazs, G. C.; del Guerzo, A.; Schmehl, R. H. *Photochem. Photobiol. Sci.* **2005**, *4*, 89–94.
(31) Michalec, J. F.; Bejune, S. A.; McMillin, D. R. *Inorg. Chem.* **2000**, *39*, 2708–2709.
(32) Pomestchenko, I. E.; Luman, C. R.; Hissler, M.; Ziessel, R.; Castellano, F. N. *Inorg. Chem.* **2003**, *42*, 1394–1396.
(33) Wang, X. Y.; Del Guerzo, A.; Schmehl, R. H. *J. Photochem. Photobiol., C* **2004**, *5*, 55–77.
(34) Schmehl, R. *Spectrum* **2000**, *13*, 17–21.
(35) Leidner, C. R.; Murray, R. W.; Meyer, T. J. *Inorg. Chem.* **1987**, *26*, 882–891.
(36) Wang, X.-Y.; Del Guerzo, A.; Schmehl, R. H. *Chem. Commun.* **2002**, 2344–2345.
(37) Klassen, D. M.; Crosby, G. A. *J. Chem. Phys.* **1968**, *48*, 1853–1858.
(38) Odongo, O. S.; Heeg, M. J.; Chen, Y. J.; Xie, P.; Endicott, J. F. *Inorg. Chem.* **2008**, *47*, 7493–7511.
(39) Gutmann, V. *The Donor Acceptor Approach to Molecular Interactions*, *Springer*, New York, 1978.

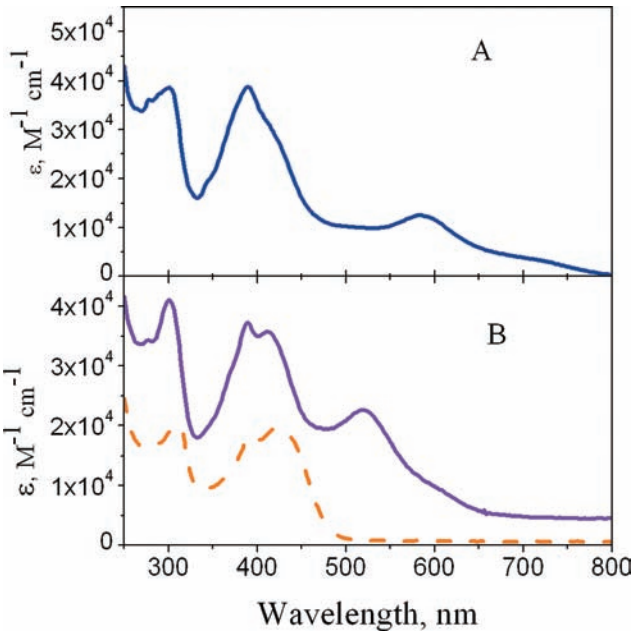

Figure 4. UV−vis absorption spectra in CH_3CN of (A) $[Ru(pyrv\text{-}bpy)_2Cl_2]$ and (B) $[Zn(pyrv\text{-}bpy)_3]^{2+}$ (yellow ---, $\varepsilon/5$) and $[Ru(pyrv\text{-}bpy)_2en]^{2+}$ (purple −).

Table 1. Electronic Spectral Data and Potentials for One-Electron Oxidation of the Ligands and Complexes in Room-Temperature Acetonitrile

compound	Abs λ_{max}, nm (log ε)	E^0(ox) V vs SCE	trans. Abs τ, ns
pyrv-bpy	290 (4.50)	1.4[a]	
	390 (4.65)		
pyr-bpy	280 (4.65)	1.6[a]	
	342 (4.41)		
$[(bpy)_2RuCl_2]$	288 (4.66)	0.31[b]	<10
	376 (4.20)		
	550 (4.19)		
$[(pyrv\text{-}bpy)_2RuCl_2]$	300 (4.59)	0.21	620
	390 (4.41)	1.4[a]	
	582 (4.10)		
$[(pyrv\text{-}bpy)_2Ru(en)]^{2+}$	300 (4.61)	0.97[a]	750
	412 (4.55)	1.4[a]	
	520 (4.35)		
$[(pyrv\text{-}bpy)_3Zn]^{2+}$	312		
	424		
$[(pyr\text{-}bpy)_2RuCl_2]$	344 (4.56)	0.3	<10
	564 (4.11)	1.6[a]	

[a] Irreversible; anodic peak potential reported; from ref 24. [b] Tanaka, M.; Nagai, T.; Miki, E. *Inorg. Chem.* **1989**, *28*, 1704.

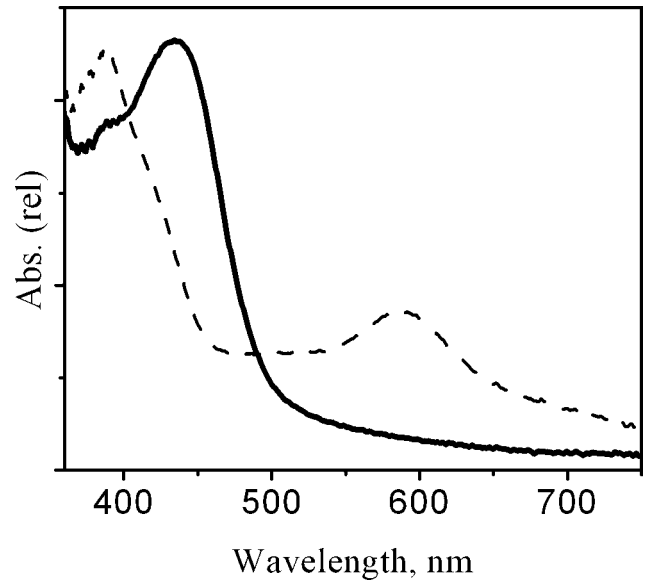

Figure 5. Acetonitrile UV−vis spectra of $[(pyrv\text{-}bpy)_2Ru(II)Cl_2]$ (---) and $[(pyrv\text{-}bpy)_2Ru(III)Cl_2]^+$ (−) obtained by oxidation at +0.5 V vs SCE.

process, preventing the determination of the molar absorptivity of the Ru(III) species, but reduction clearly led to the appearance of the original absorption spectrum (diminished somewhat because of precipitate formation).

Voltammetric analysis of complex $[(pyrv\text{-}bpy)_2Ru(en)]^{2+}$ between 0 and +1.8 V versus SCE revealed two irreversible oxidative waves. In contrast to the cis-chloro complexes, no reversible ruthenium-based oxidation was observed. The more positive oxidation wave corresponded closely to the pyrene-localized oxidation observed in $[(pyrv\text{-}bpy)_2RuCl_2]$. The lower potential oxidation, with a peak potential of 0.97 V, is attributed to the oxidation of the coordinated ethylenediamine (en) ligand. This assignment is based upon the report of Meyer and co-workers indicating that $[(bpy)_2Ru(en)]^{2+}$ is quasi-reversibly oxidized in acetonitrile. Exhaustive electrolysis indicates that each coordinated amine is oxidized to an imine as shown in Scheme 2.[40] Although we have not isolated the resulting imine complex resulting from the multielectron oxidation of $[(pyrv\text{-}bpy)_2Ru(en)]^{2+}$, our thinking at this time is that the irreversibility of the oxidation results in the same chemistry as that of the unsubstituted bipyridine complex reported by Meyer and co-workers.

Excited-State Behavior. A detailed account of the luminescence behavior of $[(bpy)_2RuCl_2]$ and $[(bpy)_2Ru(en)]^{2+}$ in frozen

Table 2. Calculated and Experimental Values for Hydrocarbon, Ligand, and Complex Singlet−Triplet Energy Gaps and Comparison with Experimental Values[a]

ligand/complex (solvent)	E singlet (hartrees)	E triplet (hartrees)	ΔE (S−T) (cm^{-1})	ΔE (nm)	% error
pyrene	−615.7731	−615.6958	16 863[b]	593	0
			16 863 (exp)	593 (exp)	
stilbene	−540.7099	−540.6315	17 480[b]	572	1.1
			17 200 (exp)	581(exp)	
pyrv-phenyl (1-styryl-pyrene)	−924.2164	−924.1497	14 660[c]	682	2.3
			14 300 (exp)	699 (exp)	
Pyrv-bpy	−1226.6896	−1226.6236	14 440	690	
$[Zn(pyvmb)(NH_3)_4]^{2+}$	−1500.3447	−1500.2995	10 580	945	
$[(bpy)_2RuCl_2]$ (EtOH)	−1114.6422	−1114.5825	13 100	763	8.4
			14 283 (exp)	700 (exp)	
$[(bpy)_2Ru(en)]^{2+}$ (CH_3CN)	−1274.91049	−1274.07165	15 725	636	4.0
			15 110 (exp)	662 (exp)	

[a] Values are based upon the energies of geometry-optimized structures for the ground-state singlet and triplet states. See the text. [b] From Murov, V. *Handbook of Photochemistry*; Dekker: New York, 1973; p 27. [c] From Arai, T.; Tokumaru, K. *Chem. Rev.* **1993**, *93*, 23.

Scheme 2. Irreversible en Oxidation in $[(bpy)_2Ru(en)]^{2+}$

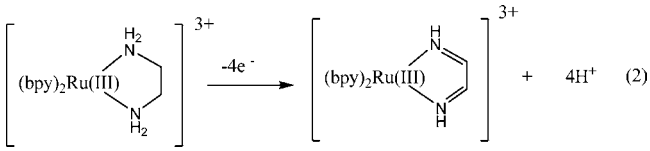

Table 3. Spectral Characteristics of $[(pyrv\text{-}bpy)_2RuCl_2]$ in Various Solvents at Room Temperature

solvent	IL maximum nm (ε, $M^{-1}cm^{-1}$)	MLCT maximum nm (ε, $M^{-1}cm^{-1}$)	τ (TA), ns
benzonitrile	394 (2.53×10^4)	606 (1.51×10^4)	322
acetonitrile	390 (2.56×10^4)	580 (1.72×10^4)	620
n-butyronitrile	388 (2.58×10^4)	582 (1.718×10^4)	535
acetone	390 (2.56×10^4)	588 (1.700×10^4)	7.6
DMF	394 (2.53×10^4)	586 (1.706×10^4)	10

matrices was reported recently by Endicott and co-workers[13] and was also described by Crosby and Klassen in the late 1960s.[41] The reported emission maxima of $[(bpy)_2RuCl_2]$ and $[(bpy)_2Ru(en)]^{2+}$ were 14 280 cm^{-1} (700 nm) and 15 110 cm^{-1} (662 nm), respectively; these values are close to those reported earlier by Crosby and Klassen.[41] Excited-state lifetimes were not reported. We examined the transient absorption spectra in solution at room temperature for $[(bpy)_2RuCl_2]$ using nanosecond laser flash photolysis. Transient spectra at different times after excitation are shown in Figure 6. The spectrum exhibits the absorption of the excited state between 350 and 400 nm and bleaching of the ground state absorption in the visible. The ground-state bleaching is clearly observed by comparison of the transient spectrum with the UV−vis spectrum of the complex, also shown in Figure 6. The excited-state absorption is similar to that reported for $[Ru(bpy)_3]^{2+}$, which has been assigned as absorption of the bipyridine anion radical associated with the ^{3}MLCT state of the complex.[42,43] The similarity of the spectrum of $[(bpy)_2RuCl_2]$ to that of the tris-bipyridine complex suggests that the state observed in the transient difference spectrum is the ^{3}MLCT state. The lifetime of this state is <10 ns and is not clearly resolvable with our equipment.

The transient difference spectrum of $[(pyrv\text{-}bpy)_2RuCl_2]$ sharply contrasts with that of $[(bpy)_2RuCl_2]$. As can be seen in Figure 7, the spectrum exhibits excited-state absorption in the UV and throughout the visible; bleaching of the ground-state absorbance is observed only at wavelengths near the maximum of the UV−vis spectrum. In addition, the excited-state lifetime in N_2-purged acetonitrile is 620 ns, which is at least 60 times longer than the lifetime of $[(bpy)_2RuCl_2]$ under similar conditions. The transient spectrum resembles that of numerous other Ru(II) diimine complexes having aromatic hydrocarbon substituents. The lowest-energy excited state of these complexes is proposed to be either a ligand-localized $^3\pi-\pi^*$ state or a triplet intraligand charge-transfer (^{3}ILCT) state. The assignments

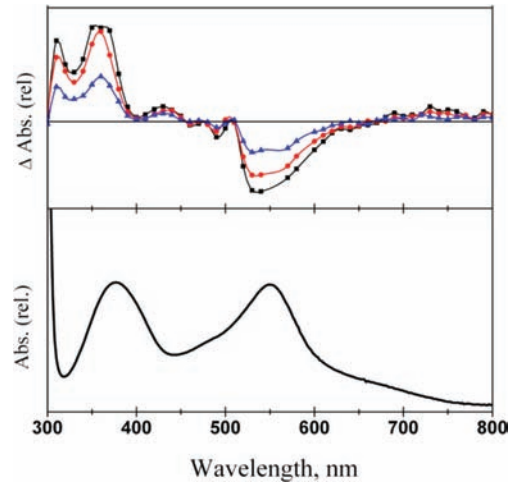

Figure 6. Transient difference spectra of $[(bpy)_2RuCl_2]$ in CH_3CN solution at room temperature at 18 (-■-), 20 (-●-), and 22 ns (-▲-) following excitation at 550 nm. The lower trace shows the UV−vis spectrum of the complex in acetonitrile.

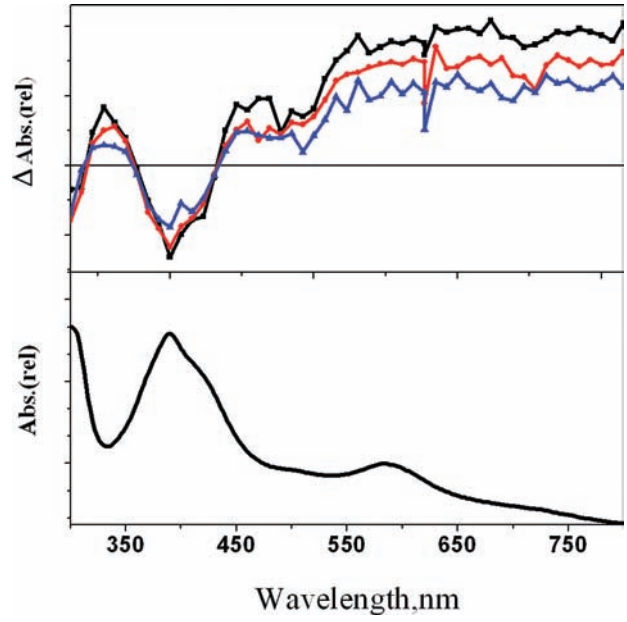

Figure 7. Transient difference spectra of $[(pyrv\text{-}bpy)_2RuCl_2]$ in CH_3CN solution at room temperature at 144 (-■-), 507 (-●-), and 640 ns (-▲-) following excitation at 550 nm. The lower trace shows the UV−vis spectrum of the complex in acetonitrile.

are often based on the relationship of the reported diimine-linked aromatic hydrocarbon $^3\pi-\pi^*$ state energy (from phosphorescence) to the energy of the ^{3}MLCT state of closely related "parent" chromophores that are luminescent. In this system, the energy of the ^{3}MLCT state is approximated from Endicott's recent publication of the emission of $[(bpy)_2RuCl_2]$.[13] However, we have not been able to obtain either room-temperature or 77 K phosphorescence spectra of $[(pyrv\text{-}bpy)_2RuCl_2]$, the pyrv-bpy ligand, or the Zn(II) complex of the pyrv-bpy ligand. As a result, we lack a definitive measure of the energy for the ligand-localized triplet state. To address this problem, the energies of the ligand-localized triplet states were estimated via density functional methods described below.

The ethylenediamine complex $[(pyrv\text{-}bpy)_2Ru(en)]^{2+}$ also exhibits transient behavior indicating that the lowest-energy excited state is ligand-localized. Figure 8 illustrates the transient

(40) Brown, G. A.; Weaver, T. R.; Keene, R. F.; Meyer, T. J.; Keenan, W. R. J. *Inorg. Chem.* **1976**, *15*, 190–196.
(41) Klassen, D. M.; Crosby, G. A. *J. Chem. Phys.* **1968**, *48*, 1853–1855.
(42) Creutz, C.; Chou, M.; Netzel, T. L.; Okumura, M.; Sutin, N. *J. Am. Chem. Soc.* **1980**, *102*, 1309–1319.
(43) Bensasson, R.; Salet, C.; Balzani, V. *J. Am. Chem. Soc.* **1976**, *98*, 3722–3724.

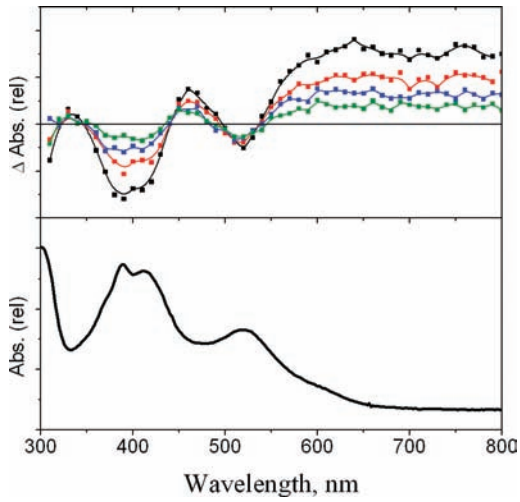

Figure 8. Transient difference spectra of $[(pyrv\text{-}bpy)_2Ru(en)]^{2+}$ in CH_3CN solution at room temperature at 130 (black -□-), 450 (-●-), 840 (blue -□-), and 1300 ns (green -□-) following excitation at 550 nm. The lower trace shows the UV−vis spectrum of the complex in acetonitrile.

difference and ground-state spectra for this complex in room-temperature CH_3CN. This complex also has bleaching at wavelengths where ground-state absorbance is strongest and excited-state absorbance at wavelengths longer than 550 nm.

Triplet-State Energy Approximation via Quenching Studies and Density Functional Methods. A key difficulty in characterizing the lowest-energy long-lived excited state of these complexes is the fact that we have not directly observed phosphorescence for the pyrv-bpy ligand or either of the complexes. In addition, attempts to obtain the ligand triplet state energy using time-resolved photoacoustic calorimetry (via collaboration) yielded no definitive energy. As a result, we have employed triplet quenching kinetic measurements and hybrid density functional calculations to bridge the gap between structurally related systems with known triplet excited-state energies and the pyrv-bpy complexes reported here. Triplet quenching studies were carried out on the coordinated ligand in the complex $[(pyrv\text{-}bpy)_2RuCl_2]$ because no triplet formation was observed upon direct photolysis of the ligand; thus, the assumption is made that the triplet energy of this complex is the same as the triplet energy of the ligand. Rate constants for quenching of the transient absorption of the complex with tetracene ($E_T = 10\,250$ cm^{-1}), perylene ($E_T = 12\,400$ cm^{-1}), and 9,10-dibromoanthracene ($E_T = 14\,060$ cm^{-1}) were found to be 3×10^9, 2×10^9, and 2×10^7 M^{-1} s^{-1}, respectively. No quenching was observed with anthracene ($E_T = 14\,900$ cm^{-1}). The implication is that the triplet-state energy is between 12 500 and 14 000 cm^{-1}. On the basis of the luminescence results of Endicott, the excited state of the complex is almost certainly lower than that of the ^{3}MLCT state of the parent complex $[(bpy)_2RuCl_2]$ (>14 000 cm^{-1}). With the limited number of data points, we decided not to fit the data to a kinetic free-energy dependence in an attempt to determine the triplet energy.

The computational approach employed was to estimate the ligand ground state−lowest-energy triplet state zero−zero energies using the hybrid B3LYP functional with an intermediate basis set of 6-31G(d,p).[44] The energy difference was taken as the difference in energy of the gas-phase or solution-optimized geometries of the two states. Although this method is very simple, it provides reliable values of the triplet-state energies for the structurally related aromatic hydrocarbon references used. Table 2 lists calculated and experimental values for three aromatic hydrocarbons as well as calculated values for pyrv-bpy and a Zn(II) complex containing pyrv-bpy, $[(NH_3)_4Zn(pyrv\text{-}bpy)]^{2+}$. The triplet energy for the Zn(II) complex was calculated because the lowest-energy state is ligand-localized but reflects an increased degree of pyrene-to-bipyridine charge-transfer interaction following the coordination of the bipyridine ligand to Zn(II). The result is that the triplet energy of the pyrv-bpy coordinated to Zn(II) is significantly lower than the triplet energy of the free ligand.

For the Ru(II) complexes, two approaches were employed to estimate excited-state energies. A method similar to that for the ligands was used, except that the ground state and lowest-energy triplet were calculated for the complex in the presence of solvent (using a polarized continuum model of Gaussian 03). The hybrid B3LYP functional was used, and the basis set was LANL2DZ for all of the atoms. We were unable to use a higher-level basis set for the lighter elements because the computation times became prohibitively long. By calculating the energies of the solvated singlet and lowest-energy triplet, a measure of the zero−zero energy is obtained. Our experience using this method with various tris-diimine chromophores of known emission energy is that the energy calculated in this way is higher than the experimental luminescence maximum energy by 0.22 ± 0.04 eV (1870 cm^{-1}). In the case of the cis-chloro complex, the computationally determined energy is lower than the experimental energy reported by Endicott (Table 2).

An alternate approach to estimating the energy of the lowest-energy triplet was via time-dependent density functional calculations on the geometry-optimized singlet ground states of the chromophores. In this case also, the method used was B3LYP and the basis set for the light elements was 6-31G(d,p) whereas that for Ru and Cl was LANL2DZ. Time-dependent DFT calculations for the ground-state optimized geometry included acetonitrile solvent using the polarized continuum model included with Gaussian 03. The result provides a measure of the vertical transition energies for the complexes (ground-state singlet to lowest-energy triplet vertical transitions). For $[(bpy)_2RuCl_2]$, the lowest-energy transition is at 690 nm (14 500 cm^{-1}), slightly higher than the experimental value (Table 2). The orbitals of the transition (from the CI coefficient expansions) clearly indicate the lowest singlet−triplet transition to be Ru dπ to bpy π* MLCT. The ground-state to lowest-energy triplet transition for the en complex, $[(bpy)_2Ru(en)]^{2+}$, is also higher in energy than the experimental values at 602 nm (16 600 cm^{-1}), and as with the cis-chloro complex, the transition is very clearly MLCT. Time-dependent analysis of the $[(bpy)(pyrv\text{-}bpy)RuCl_2]$ complex indicates that the transition to the lowest-energy triplet lies at 750 nm (13 300 cm^{-1}), which is in the middle of the triplet energy range derived from triplet quenching experiments (vide supra). For this molecule, the CI coefficient expansion indicates that the transition has contributions from MLLCT, Ru dπ to Pyrv-bpy π*, and a rather diffuse dπ, Pyrv-bpy π-to-Pyrv-bpy π* transition. The influence of the styryl pyrene substituent is readily apparent in lowering the energy of the transition and in increasing the degree of ligand localization in the transition.

The calculations help support the concept that the lowest-energy transition on the pyrv-bpy containing complexes is, to a significant extent, localized on the pyrv-bpy ligand. In addition,

(44) Frisch, M. J., et al. *Gaussian 03, Revision D.02*; Gaussian, Inc.: Wallingford, CT, 2004.

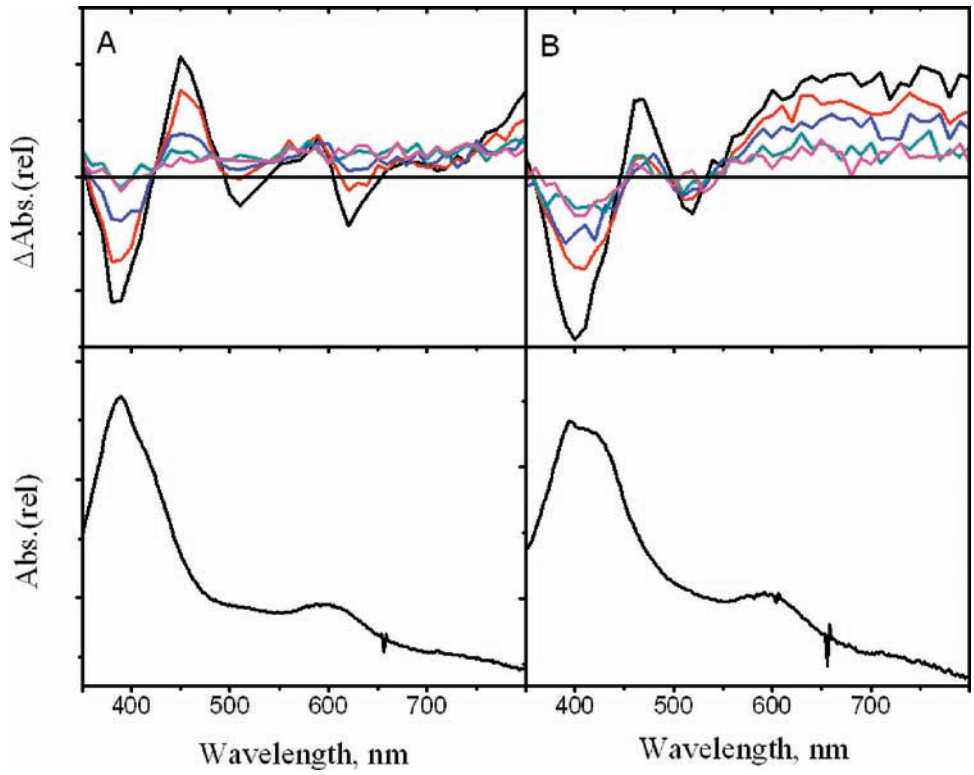

Figure 9. Transient difference spectra of $[(pyrv\text{-}bpy)_2RuCl_2]$ in (A) acetone between 10 and 30 ns and (B) benzonitrile between 20 and 500 ns.

the energy gap between this lowest-energy triplet state and the higher-energy MLCT state is certainly greater for the en complex than for the cis-chloro complex.

Solvatochromism in Transient Spectra of $[(pyrv\text{-}bpy)_2RuCl_2]$. The electronic spectra of $[(bpy)_2RuCl_2]$ exhibit solvatochromism in the Ru-to-bpy MLCT transition. A question that arises relates to the relative energy of MLCT and ligand-localized excited states as a function of solvent. Figure 9 shows spectra of the complex in benzonitrile and acetone; the benzonitrile spectrum clearly shows the transient spectrum indicative of the ligand-localized excited state. The difference spectrum in acetone has a very short excited-state lifetime and bleaching of the MLCT absorption between 550 and 600 nm and a unique transient absorbance at 470 nm. In all of the nitrile solvents examined, the transient spectrum reflects a ligand-localized excited state (long lifetime and TA with strong absorbance in the red) whereas in acetone and DMF the photoactive excited state was MLCT (short lifetime with 470 nm absorbance and bleaching in the green). The spectrum in benzonitrile (Figure 9B) shows that, within a few nanoseconds of laser excitation, a short-lived absorbance feature at 470 nm is observed that yields to the longer-lived ligand-localized triplet transient spectrum. The complex is soluble in only a limited number of solvents, and it was not possible to make a meaningful correlation of the relative-state energy with the solvent donor number or other solvent parameters. A final note relating to this is that the photolysis of the complex in CH_2Cl_2 resulted in a color change from green to yellow; the final spectrum is similar to that of the one-electron oxidized complex (Figure 5). The implication of this observation is that the photoexcited pyrv-bpy complex is capable of reducing the solvent, although we have not examined this in detail.

Photoinduced Electron Transfer of $[(pyrv\text{-}bpy)_2RuCl_2]$ to Electron Acceptors. The energy of the ligand-localized excited state of $[(pyrv\text{-}bpy)_2RuCl_2]$ can be approximated from density functional results for the Zn(II) complex of pyrv-bpy (Table 2) to be 1.3 eV (10 500 cm^{-1}). If the excited state of the complex is ligand-localized and the excited state is to be used in the reduction of an electron acceptor, then a question that arises as to whether the oxidation of the chromophore will occur on the ligand or at the more easily oxidized metal center. There is a very large difference in the potentials for oxidation of the pyrv-bpy ligand (~1.4 V) and the Ru(II) center (0.2 V). If excited-state electron transfer initially results in the oxidation of the pyrv-bpy ligand, then the excited state will be a very weak reducing agent. If we use 1.3 eV as the energy of the pyrv-bpy ligand-localized state and 1.4 V versus SCE as the E^0 for the one-electron reduction of the coordinated pyrv-bpy ligand cation radical, then the potential for oxidation of the excited state (eq 1) is negative and the ligand-localized excited state should not be able to reduce methyl viologen.

$$[(pyrv^{+\bullet}\text{-}bpy)_2Ru(II)Cl_2] + e^- \rightleftharpoons [(pyrv\text{-}bpy)(^*pyrv\text{-}bpy)Ru(II)Cl_2] \quad E^0 \approx 0.1\ V \quad (1)$$

If, however, the excited-state electron transfer involves the direct oxidation of Ru(II), then the excited-state potential (eq 2), as expressed below, may be as positive as +1.1 V versus SCE.

$$[(pyrv\text{-}bpy)_2Ru(III)Cl_2] + e^- \rightleftharpoons (pyrv\text{-}bpy)(^*pyrv\text{-}bpy)Ru(II)Cl_2] \quad E^0 \approx -1.1\ V \quad (2)$$

To address this question, we examined the quenching of the transient absorbance of $[(pyrv\text{-}bpy)_2RuCl_2]$ with a variety of electron-accepting quaternary ammonium salts in acetonitrile. Rate constants, given in Table 4, are all greater than $10^8\ M^{-1}\ s^{-1}$ except for that for quencher 5 ($E^0 = -1.1$ V vs SCE), which was somewhat slower. Thus, quenching is still facile for electron acceptors with a potential of −0.65 V (quencher 4), clearly

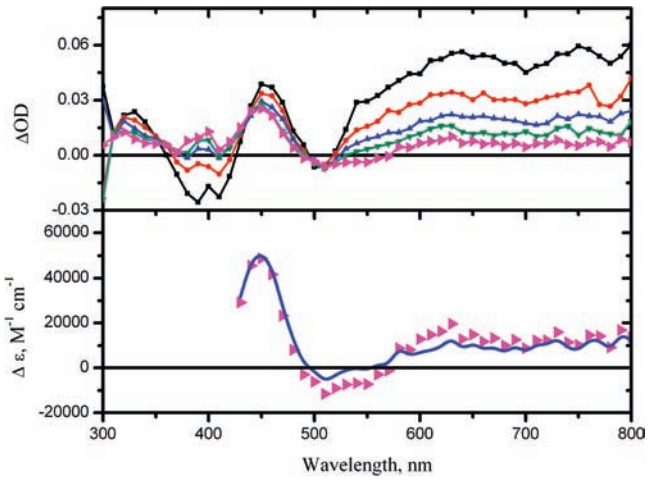

Figure 10. Transient spectrum of the cis chloro complex in the presence of 5 mM methyl viologen in nitrogen-purged acetonitrile at different times after excitation between 50 ns and 500 ns. The final spectrum represents the spectrum of the charge-separated species. The lower frame represents a comparison of the experimental (triangles) and calculated transient spectrum (solid line) of the radical ion products generated using the method described in the text.

Table 4. Viologen and Pyridine Compounds Used as Quenchers

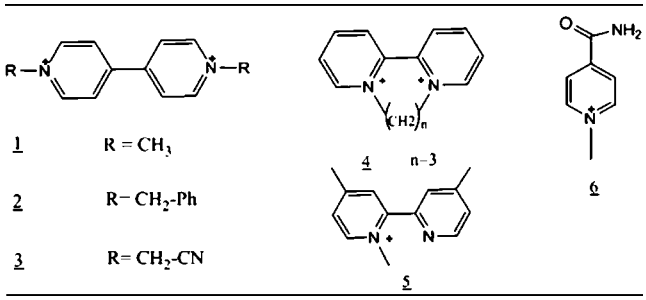

Table 5. Rate Constants for Quenching [(pyrv-bpy)$_2$RuCl$_2$] with Quaternary Ammonium Electron Acceptors in Acetonitrile at Room Temperature

quencher	$k_q \times 10^{-8}$, M^{-1} s^{-1}	E^0 (Q^{2+}/ Q^+), V vs SCE
3	6.7	−0.15
2	4.9	−0.24
1	6.81	−0.45
4	19.4	−0.66
6	1.1	−0.84
5	0.74	−1.1

indicating that the reactive excited state of the complex reacts directly to form the Ru(III) species (and not the pyrv-bpy cation radical). Further support for this is given in Figure 10, which shows the transient absorption spectrum of [(pyrv-bpy)$_2$RuCl$_2$] in acetonitrile containing 5 mM methyl viologen. The spectra obtained at different times after excitation show the disappearance of the excited state and the formation of a long-lived transient that exhibits a strong absorption transient signal at 440 nm and small signals for absorption between 350 and 400 nm, bleaching between 500 and 550 nm, and weak absorbance further to the red. In general, photoinduced electron transfer involving methyl viologen results in a strong absorbance transient at 390 nm and broad absorption between 570 and 700 nm. In this case, the ground-state absorption of the Ru complex chromophore is very similar to that of reduced methyl viologen and thus the absorbance of reduced viologen is nearly completely offset by the bleaching of the oxidized Ru complex. The lower segment of Figure 10 shows the experimental spectrum of the radical ion products and the spectrum calculated by first generating the spectrum of the known components (the reduced viologen minus the ground-state Ru(II) complex), assuming the transient spectrum of the radical ion products at 600 nm consists of only reduced viologen and bleached Ru(II), using the absorptivity to calculate the concentration of radical ions, and finally using this concentration to generate the transient difference spectrum in terms of molar absorptivity. The result is that the transient absorbance data provides direct evidence that quenching of the reactive excited state of [(pyrv-bpy)$_2$RuCl$_2$] by electron acceptors results in the formation of the one-electron-oxidized Ru complex because the transient species absorbing at 440 nm mirrors that of the one-electron-oxidized Ru complex observed spectroelectrochemically. It should be noted that, although complexes [(bpy)$_2$RuCl$_2$] and [(bpy)$_2$Ru(en)] do not produce radical ions with low concentrations of acceptors such as viologens (5 mM or less), it is possible to observe photoredox products with these chromophores using a much higher quencher concentration (∼0.1 M).

Summary

This work demonstrates that multichromophoric molecules having a visible-light-absorbing MLCT component coupled to a UV-absorbing ligand-localized excited state of the same spin multiplicity can result in sensitization of the ligand-localized state. The result is an excited state with a lifetime long enough to undergo bimolecular electron-transfer reactions, as opposed to the MLCT state of the unmodified complex. With complex [(pyrv-bpy)$_2$RuCl$_2$], the pyrv "localized" excited state formed reacts via photoinduced electron transfer with a variety of electron acceptors. The remarkable aspect of the electron-transfer process is that, whereas the excited state can be considered to be ligand-localized, the photoredox reaction almost certainly involves the direct formation of the one-electron-oxidized metal center.

Experimental Section

Materials. All starting materials were purchased either from Aldrich or Strem Chemicals and were used without further purification. All solvents, including NMR solvents, were used as obtained. Acetonitrile for electrochemistry was dried by refluxing over CaH_2 under a N_2 atmosphere and distilled immediately before use. Dimethylformamide (DMF) for electrochemistry was dried over P_2O_5 overnight and distilled immediately prior to use. Silica columns were run in the open air using 32−63 μm silica.

Spectroscopy. NMR spectra were recorded on a Varian 400 MHz NMR. Chemical shifts are referenced internally to the solvent signal. All UV−vis absorption spectra were obtained on a Hewlett-Packard 8452A diode array spectrophotometer. ESI mass spectra were obtained using a Bruker microTOF spectrometer.

Electrochemistry. Cyclic voltammetry and differential pulse voltammetry were obtained using a CH Instruments 630 electrochemical workstation. The complexes were dissolved in freshly distilled, nitrogen-purged solvent with 0.1 M tetrabuylammonium hexafluorophosphate (TBAH) as the supporting electrolyte. The working electrode was a freshly polished glassy carbon disk (0.2 cm^2). Potentials were measured versus a nonaqueous Ag/Ag^+ reference electrode (CH Instruments) but also included ferrocene is as an internal reference. Spectroelectrochemical analysis was carried out using the CH Instruments workstation for potential control and an Ocean Optics USB 2000 spectrophotometer for spectrophotometric analysis. The cell for spectroelectrochemical measurements was home-built, featuring a 0.2 cm path length and

a Pt grid working electrode (50 lines/in) at a Pt coil counter electrode and a Ag wire pseudoreference.

Time-Resolved Transient Absorption Spectra. Transient absorption measurements were performed using a Brilliant B Q-switched Nd:YAG laser-pumped OPO (Opotek) as the pump source at a right angle to the analyzing light source. Excitation pulses were generally <5 ns between 410−600 nm. An Applied Photophysics LKS.60 laser flash photolysis spectrometer was used for detection; the instrument is equipped with a 150 W pulsed Xe lamp as the analyzing light source, a single grating monochromator after the sample, and PMT detection. The output was recorded on an Agilent Infiniium transient digitizer and analyzed with Applied Photophysics LKS.60 software.

Syntheses. The preparation of $[(bpy)_2RuCl_2]$ and $[Ru(bpy)_2(en)](PF_6)_2$ followed modifications of literature procedures and is included in the Supporting Information.[38,40]

4-(Pyrenylvinyl)-4′-methyl-2, 2′-bipyridine (pyrv-bpy).[45] Potassium *tert*-butoxide (0.23 g, 2 mmol) was added to a THF (20 mL) solution of 1-pyrenecarboxaldehyde (0.23 g, 0.99 mmol) and **2** (0.30 g, 0.937 mmol). The resulting mixture was allowed to stir for 24 h at ambient temperature. The solvent was then removed under reduced pressure. The crude residue was dissolved in a minimal volume of dichloromethane and dispersed in 30 mL of hexane. The precipitate was collected by filtration and washed with distilled water (3 × 5 mL), followed by ether (3 × 5 mL). This gave 0.18 g of light-yellow product **3** (yield 48.5%). ^{1}H NMR: δ 8.70 (d, J_{H-H} = 4.5 Hz, 1H), 8.67 (s, 1H), 8.60 (d, J_{H-H} = 4.5 Hz, 1H), 8.53 (dd, $J_{vinyl\text{-}H-H}$ = 16 Hz, J_{H-H} = 6.8 Hz, 2H), 8.33 (d, J_{H-H} = 8 Hz, 1H), 8.29 (s, 1H), 8.21−8.19 (m, 4H), 8.08 (d, J_{H-H} = 2.4 Hz, 2H), 8.015 (t, J_{H-H} = 8 Hz, 1H), 8.54 (d, J_{H-H} = 4.5 Hz, 1H), 7.36 (d, $^3J_{vinyl\text{-}H-H}$ = 16 Hz,1H), 7.18 (d, J_{H-H} = 4.5 Hz, 1H), 2.47 (s, 3H).

$[(pyrv\text{-}bpy)_2RuCl_2]$.[35] A 12 mg (0.05 mmol) sample of $RuCl_3 \cdot 3H_2O$ was mixed with 40 mg (0.1 mmol) of **3** and 8 mg(0.189 mmol) of LiCl in a round-bottomed flask, and 10 mL of $CH_3OCH_2CH_2OH$ was added. After heating to 125 °C with stirring for 8 h under an atmosphere of argon, the reaction mixture was cooled to room temperature and placed in an ice bath overnight. The dark-brown mixture was filtered, affording a black precipitate that was washed with water (3 × 5 mL) and diethyl ether (3 × 5 mL). The crude product was redissolved in a minimal volume of DMSO and precipitated by addition to 20 mL of diethyl ether. The black-powdered product (25 mg, 52%) was collected by suction filtration. ESI mass: *m*/*e* calcd for $C_{58}H_{40}Cl_2N_4Ru$, 964.1678; found, 964.1739. (See Supporting Information for the isotope distribution.)

$[(pyrv\text{-}bpy)_2Ru(en)][PF_6]_2$.[38] A 20 mg (0.02 mmol) sample of $[Ru(pyrv\text{-}bpy)_2Cl_2]$ was suspended in 10 mL of 1:1 (v/v) water−methanol followed by the addition of 80 mg (1.33 mmol) of ethylene diamine (en). The resulting mixed solution was refluxed at 100 °C for 2 h under an atmosphere of argon. After cooling to room temperature, 5 mL of a saturated aqueous solution of NH_4PF_6 was added to the reaction mixture. The red precipitate that formed was collected by suction filtration and washed with distilled water (3 × 5 mL), followed by diethyl ether (3 × 5 mL). The black-powdered product (11 mg, 44%) was obtained by filtration. ESI Mass: *m*/*e* calcd for $C_{60}H_{48}N_6Ru$, 477.1494; found, 477.1548.

Acknowledgment. We thank the U.S. Department of Energy, Office of Chemical Sciences (grant DE-FG-02-96ER14617) for supporting this research. We also thank the National Science Foundation (grant CHE0619770) for funding for the ESI mass spectrometer. J.G. thanks the IBM Corporation for a fellowship in Computational Science administered through the Tulane Center for Computational Science.

Supporting Information Available: Detailed syntheses, ^{1}H NMR and mass spectral data, sample Stern−Volmer quenching data, and extended references. This material is available free of charge via the Internet at http://pubs.acs.org.

JA909785B

(45) Viau, L.; Maury, O.; Le Bozec, H. *Tetrahedron Lett.* **2004**, *45*, 125–130.